Reprinted from March 1988, Vol. 110, Journal of Applied Mechanics

Nonlinear Composite Beam Theory

O. A. Bauchau
Assistant Professor.

C. H. Hong
Graduate Assistant.

Department of Mechanical Engineering,
Aeronautical Engineering and Mechanics,
Rensselaer Polytechnic Institute,
Troy, New York, 12180-3590

The modeling of naturally curved and twisted beams undergoing arbitrarily large displacements and rotations, but small strains, is a common problem in numerous engineering applications. This paper has three goals: (1) present a new formulation of this problem which includes transverse shearing deformations, torsional warping effects, and elastic couplings resulting from the use of composite materials, (2) show that the small strain assumption must be applied in a consistent fashion for composite beams, and (3) present some numerical results based on this new formulation to assess its accuracy, and to point out some distinguishing feature of anisotropic beam behavior. First, the predictions of the formulation will be compared with experimental results for the large deflections and rotations of an aluminum beam. Then, the distinguishing features of composite beams that are likely to impact the design of rotating blades (such as helicopter blades) will be discussed. A first type of extension-twisting coupling introduced by the warping behavior of a pretwisted beam is discussed, then, a shearing strain squared term, usually neglected in small strain analyses, is shown to introduce a coupling between axial extension and twisting behavior, that can be significant when the ratio E/G *is large (*E *and* G *are Young's and shearing moduli of the beam, respectively). Finally, the impact of inplane shearing modulus changes and torsional warping constraints on the behavior of beams exhibiting elastic couplings is investigated.*

1 Introduction

The nonlinear static and dynamic analysis of naturally curved and twisted beams has received considerable attention in recent years (Friedmann, 1977; Rosen, 1979; Rosen et al., 1987; Bauchau et al., 1987c), and has many important applications in aeronautical engineering such as helicopter blades and flexible space structures. The nonlinear kinematics involved in this problem are complex since both deformed and undeformed configurations of the beam are three-dimensional. Moreover, laminated composite materials are increasingly used for the construction of such structures, causing several nonclassical effects of beam theory to become more pronounced, such as transverse shearing deformations, torsion related warpings (Bauchau et al., 1985, 1987a), and elastic couplings.

The assumption of indeformability of the cross-section in its own plane is fundamental in beam theory as it reduces a three-dimensional problem to a one dimensional model along the axis of the beam. In the Euler-Bernoulli theory, cross sections are assumed to remain plane during deformation, however, with anisotropic materials, out-of-plane warping can become important, and torsion related warpings should be included in the analysis. In many applications, large deflections and rotations of the beam will occur, however the strain level remains low. For instance, in a helicopter blade fatigue life is a major concern, hence the operating strain level must remain well within the linear-elastic range of the material. As a result, most analyses (Rosen et al., 1979, 1987; Bauchau et al., 1987b, 1987c) are based on a small strain assumption that considerably simplifies the formulation and the resulting equations.

The small strain assumption has important implications. First, the Green-Lagrange strain components often used in the derivation of the nonlinear kinematics (Rosen et al., 1979, 1987) can be equated to the engineering strain components, and hence the usual stress-strain relationships of the material can be used. Second, the changes in surface area of a differential volume element due to deformation are negligible, and finally the strain-displacement equations can be considerably simplified since all second order terms (i.e, strain square terms) can be neglected.

The objective of this paper is to present a consistent, nonlinear analysis of naturally curved and twisted beams undergoing arbitrarily large deflections and rotations. Transverse shearing deformations, torsional warping effects, and elastic couplings resulting from the use of composite materials are all included in the formulation. Numerical results based on a finite element approximation of the resulting equations are presented. Special attention is devoted to the extension twisting behavior of composite beams which is important to the design of aeroelastically tailored composite helicopter blades.

2 Geometry of the Beam and Kinematics of the Deformation

Consider the naturally curved and twisted beam depicted in

Contributed by the Applied Mechanics Division for publication in the Journal of Applied Mechanics.

Discussion on this paper should be addressed to the Editorial Department, ASME, United Engineering Center, 345 East 47th Street, New York, N.Y. 10017, and will be accepted until two months after final publication of the paper itself in the Journal of Applied Mechanics. Manuscript received by ASME Applied Mechanics Division, April 1, 1987; final revision October 9, 1987.

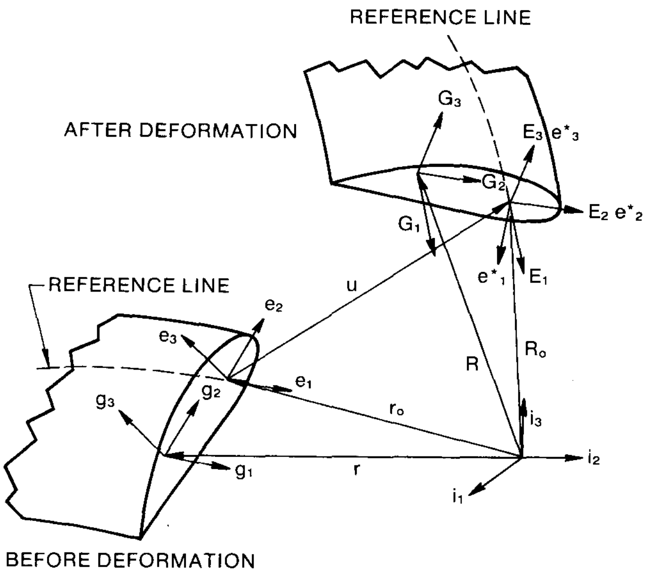

Fig. 1 Geometry of the beam before and after deformation

Fig. 1. The triad $\mathbf{i}_1, \mathbf{i}_2, \mathbf{i}_3$ is fixed in space and the triad $\mathbf{e}_1, \mathbf{e}_2, \mathbf{e}_3$ is attached to a reference line along the axis of the beam. $\mathbf{e}_1$ is chosen tangent to the reference line and $\mathbf{e}_2, \mathbf{e}_3$ define the plane of the cross section. The curvilinear coordinates along this triad are x_1, x_2, and x_3, respectively. The position vector of a particle of the beam in the undeformed configuration is

$$\mathbf{r} = \mathbf{r}(x_1, x_2, x_3). \tag{1}$$

After deformation the same particle has a position vector

$$\mathbf{R} = \mathbf{R}(x_1, x_2, x_3) \tag{2}$$

The corresponding vectors at the reference line are

$$\mathbf{r}_0 = \mathbf{r}_0(x_1, 0, 0) \text{ and } \mathbf{R}_0 = \mathbf{R}_0(x_1, 0, 0), \tag{3}$$

and displacement vector of the reference line is given by

$$\mathbf{u} = \mathbf{R}_0 - \mathbf{r}_0. \tag{4}$$

The base vectors (Washizu, 1975; Wempner 1981) in the undeformed and deformed positions, respectively, are defined as

$$\mathbf{g}_i = \mathbf{r}_{,i} \text{ and } \mathbf{G}_i = \mathbf{R}_{,i}, \tag{5}$$

where the notation $(.)_{,i}$ means derivative with respect to x_i. At the reference line the base vectors are

$$\mathbf{e}_i = \mathbf{r}_{0,i} \text{ and } \mathbf{E}_i = \mathbf{R}_{0,i}. \tag{6}$$

$\mathbf{e}_i$ forms a triad since the derivatives in equation (6) are taken with respect to the natural coordinates of the beam. The triad $\mathbf{e}_i$ can be viewed as a rotation of the basic reference triad $\mathbf{i}_i$ through a given rotation matrix $t(x_1)$ such that:

$$\mathbf{e}_i = t^T(x_1)\mathbf{i}_i. \tag{7}$$

The derivatives of this triad are readily calculated as:

$$\begin{bmatrix} \mathbf{e}_1' \\ \mathbf{e}_2' \\ \mathbf{e}_3' \end{bmatrix} = \begin{bmatrix} 0 & k_3 & -k_2 \\ -k_3 & 0 & k_1 \\ k_2 & -k_1 & 0 \end{bmatrix} \begin{bmatrix} \mathbf{e}_1 \\ \mathbf{e}_2 \\ \mathbf{e}_3 \end{bmatrix} \tag{8}$$

where $(.)'$ means derivative with respect to x_1; k_1 is the natural twist (or pretwist), k_2 and k_3 the natural curvature (or prebend) of the beam. The position vector of an arbitrary point of the cross section can be expressed as:

$$\mathbf{r} = \mathbf{r}_0 + x_2\,\mathbf{e}_2 + x_3\,\mathbf{e}_3, \tag{9}$$

hence the base vectors become:

$$\begin{aligned} \mathbf{g}_1 &= \sqrt{g}\mathbf{e}_1 - x_3k_1\,\mathbf{e}_2 + x_2k_1\,\mathbf{e}_3, \\ \mathbf{g}_2 &= \mathbf{e}_2, \\ \mathbf{g}_3 &= \mathbf{e}_3. \end{aligned} \tag{10}$$

The metric tensor is obtained as $\mathbf{g}_{ij} = \mathbf{g}_i \cdot \mathbf{g}_j$ and its determinant is $\mathbf{g}$. The fundamental assumption in beam theory is that the cross section does not deform in its own plane. This means that the base vector $\mathbf{E}_2$ and $\mathbf{E}_3$ which are in the plane of the cross section after deformation simply correspond to a translation and rotation of the base vectors $\mathbf{e}_2$ and $\mathbf{e}_3$ of the original configuration. Note that arbitrarily large displacements and rotations can occur, but no deformation of the cross section is allowed, i.e., $\mathbf{E}_2$ and $\mathbf{E}_3$ are mutually orthogonal unit vectors. In contrast $\mathbf{E}_1$ is no longer unit nor orthogonal to $\mathbf{E}_2$ or $\mathbf{E}_3$, as axial and shearing strains are allowed. The triad $\mathbf{e}_i^*$ is defined as follows:

$$\mathbf{e}_2^* = \mathbf{E}_2,\ \mathbf{e}_3^* = \mathbf{E}_3,\ \mathbf{e}_1^* = \mathbf{e}_2^* \times \mathbf{e}_3^* \tag{11}$$

The vector $\mathbf{E}_1$ can be resolved in this triad as:

$$\mathbf{E}_1 = (1 + \bar{e}_{11})\mathbf{e}_1^* + 2\bar{e}_{12}\mathbf{e}_2^* + 2\bar{e}_{13}\mathbf{e}_3^* \tag{12}$$

At this point, $\bar{e}_{11}$, $\bar{e}_{12}$, and $\bar{e}_{13}$ are the unknown components of $\mathbf{E}_1$ along the triad $\mathbf{e}_i^*$, however they will be identified later as strain quantities. Here again the triad $\mathbf{e}_i^*$ can be related to the basic reference triad $\mathbf{i}_i$ through an unknown rotation matrix $T(x_1)$ such that:

$$\mathbf{e}_i^* = T^T(x_1)\mathbf{i}_i. \tag{13}$$

The derivatives of this triad are:

$$\begin{bmatrix} \mathbf{e}_1'^* \\ \mathbf{e}_2'^* \\ \mathbf{e}_3'^* \end{bmatrix} = \begin{bmatrix} 0 & K_3 & -K_2 \\ -K_3 & 0 & K_1 \\ K_2 & -K_1 & 0 \end{bmatrix} \begin{bmatrix} \mathbf{e}_1^* \\ \mathbf{e}_2^* \\ \mathbf{e}_3^* \end{bmatrix} \tag{14}$$

where K_1 is the twist, and K_2 and K_3 the curvatures of the deformed beam. Since the cross section does not deform in its own plane, the position vector in the deformed configuration can be written as:

$$\begin{aligned} \mathbf{R} &= \mathbf{R}_0 + x_2\mathbf{E}_2 + x_3\mathbf{E}_3 \\ &+ [\delta(x_1)W_1(x_2, x_3) + 2\hat{e}_{12}W_2(x_2, x_3) + 2\hat{e}_{13}W_3(x_2, x_3)]\mathbf{e}_1^* \end{aligned} \tag{15}$$

The first three terms represent large translations and rotations of the cross section and can be interpreted geometrically as plane sections remaining plane, but not necessarily normal to the deformed axis of the beam. The last term represents a small displacement in the direction of $\mathbf{e}_1^*$, that is out-of-plane warping of the cross section. This warping has three components: one torsion related warping displacement W_1, and two bending related warpings W_2, and W_3. These warping displacements are selected as the St. Venant warping functions (5). $\delta(x_1)$ is an unknown function characterizing the magnitude of the torsional warping, whereas the magnitude of the bending related warpings are chosen proportional to the average transverse shearing strains $2\hat{e}_{12}$ and $2\hat{e}_{13}$. Combining equations (5), (6), (12), and (14) the base vectors of the deformed configuration become:

$$\begin{aligned} \mathbf{G}_1 &= [(1+\bar{e}_{11}) - x_2K_3 + x_3K_2 + \delta' W_1]\mathbf{e}_1^* \\ &+ [2\bar{e}_{12} - x_3K_1]\mathbf{e}_2^* + [2\bar{e}_{13} + x_2K_1]\mathbf{e}_3^* \\ \mathbf{G}_2 &= [\delta W_{1,2} + 2\hat{e}_{12}W_{2,2} + 2\hat{e}_{13}W_{3,2}]\mathbf{e}_1^* + \mathbf{e}_2^* \\ \mathbf{G}_3 &= [\delta W_{1,3} + 2\hat{e}_{12}W_{2,3} + 2\hat{e}_{13}W_{3,3}]\mathbf{e}_1^* + \mathbf{e}_3^* \end{aligned} \tag{16}$$

In equations (16) all higher order terms containing warping quantities have been neglected, and differential bending related warpings are neglected as well (Bauchau et al., 1985, 1987). The Green-Lagrange strain components in a curvilinear coordinate system (Washizu, 1975) are given as

$f_{ij}=1/2(G_{ij}-g_{ij})$ where G_{ij} is the metric tensor in the deformed configuration defined as $\mathbf{G}_{ij}=\mathbf{G}_i \cdot \mathbf{G}_j$. It is straightforward to verify that $f_{22}=f_{33}=f_{23}=0$ as a direct implication of the indeformability of the cross section in its own plane. The other strain components are the transverse shearing strains $\sqrt{g}\, e_{12}=f_{12}$ and $\sqrt{g}\, e_{13}=f_{13}$, and the axial strain component $ge_{11}=f_{11}+2x_3k_1f_{12}-2x_2k_1f_{13}$, where e_{11}, e_{12}, and e_{13} are the components of the Green-Lagrange strain tensor in the local orthogonal coordinate system $\mathbf{e}_i$. The initial curvature of the beam k_2 and k_3 are now assumed to be small, hence $\sqrt{g}=1-x_2k_3+x_3k_2 \cong 1$. This assumption is realistic in many practical applications and is satisfied for helicopter blades. The strain components now become:

$$2e_{12} = 2\bar{e}_{12}-x_3\kappa_1+\delta W_{1,2}+2\hat{e}_{12}W_{2,2}+2\hat{e}_{13}W_{3,2} \quad (17)$$

$$2e_{13} = 2\bar{e}_{13}+x_2\kappa_1+\delta W_{1,3}+2\hat{e}_{12}W_{2,3}+2\hat{e}_{13}W_{3,3} \quad (18)$$

$$\begin{aligned} e_{11} = {} & \bar{e}_{11}+1/2\bar{e}_{11}^2-x_2(1+\bar{e}_{11})\kappa_3+x_3(1+\bar{e}_{11})\kappa_2+\delta' W_1 \\ & + \delta k_1(x_3W_{1,2}-x_2W_{1,3}) \\ & + 1/2(2\bar{e}_{12}-x_3\kappa_1)^2+1/2(2\bar{e}_{13}+x_2\kappa_1)^2 \\ & + 1/2(x_2\kappa_3-x_3\kappa_2)^2 \end{aligned} \quad (19)$$

where $\kappa_i=K_i-k_i$. To complete the formulation, the coefficients $\bar{e}_{11}$, $\bar{e}_{12}$, and $\bar{e}_{13}$ first introduced in equation (12) must now be related to the displacements and rotations; differentiating equation (4) with respect to x_1 and using equations (6) we obtain:

$$\mathbf{E}_1=\mathbf{e}_1+\mathbf{u}' \quad (20)$$

or

$$\mathbf{E}_1=(u_1'+t_{11})\mathbf{i}_1+(u_2'+t_{21})\mathbf{i}_2+(u_3'+t_{31})\mathbf{i}_3 \quad (21)$$

where u_i are the components of the displacement vector in the basic reference triad $\mathbf{i}_i$, and t_{ij} the components of the rotation matrix t. On the other hand, combining equations (12) and (13) yields another relation for $\mathbf{E}_1$ that can be identified with equations (21) to obtain:

$$\begin{bmatrix} 1+\bar{e}_{11} \\ 2\bar{e}_{12} \\ 2\bar{e}_{13} \end{bmatrix} = T^T \begin{bmatrix} u_1'+t_{11} \\ u_2'+t_{21} \\ u_3'+t_{31} \end{bmatrix} \quad (22)$$

This completes the strain analysis. It is important to note that this development is valid for arbitrarily large displacements, rotations, and strains. The unknowns of the problem are the three displacement components u_i, the three rotation parameters implicitly defined in the rotation matrix T, and the torsional warping amplitude.

3 Strain Energy in the Beam

The total potential energy for the present problem is:

$$\Pi=\frac{1}{2}\int_0^L\int_\Omega \sigma_{ij}e_{ij}\sqrt{g}\,d\Omega\,dx_1-W \quad (23)$$

where σ_{ij} are the components of the stress tensor measured per unit surface of the undeformed configuration and e_{ij} are the components of the Green-Lagrange strain tensor, both measured in the local coordinate system $\mathbf{e}_i$ (Washizu, 1975); W the work done by the applied loads, Ω the cross-sectional area of the beam, and L its length. We now assume that the strain components remain small enough to render negligible the changes in surface area of a differential volume element due to deformation. This situation occurs in many practical applications, such as helicopter blades. Hence, the stress components σ_{ij} can be equated to the components of the Cauchy stress tensor in the local axis system $\mathbf{e}_i$, and the Green-Lagrange strain components e_{11}, $2e_{12}$, and $2e_{13}$ become equal to the engineering strain components ϵ_{11}, γ_{12}, and γ_{13}, respectively.

At this point, we will focus on thin-walled beams which are a realistic model for helicopter blades. This is not a restrictive assumption as the present theory could be applied to a solid cross section as well. For thin-walled sections the only nonvanishing stress components are the axial and shear stress flows, n and q, respectively; hence equation (23) now becomes:

$$\Pi=\frac{1}{2}\int_0^L\int_\Gamma (n\,e+q\,\gamma)ds\,dx_1-W \quad (24)$$

where s is the curvilinear coordinate describing the thin-walled contour Γ, e is the axial strain, and γ the engineering shearing strain between a line element along the contour and one perpendicular to the cross section, given by:

$$\gamma=2e_{12}x_2^+ +2e_{13}x_3^+, \quad (25)$$

where $(.)^+$ denotes derivative with respect to s. The axial strain is given by equation (19), and the shearing strain is found by combining equations (17), (18), and (25) to obtain:

$$\gamma=2\bar{e}_{12}G_2+2\bar{e}_{13}G_3+\delta W_1^+ +\rho\,\kappa_1, \quad (26)$$

where $G_2=x_2^+ + W_2^+$ and $G_3=x_3^+ + W_3^+$ are the shearing strain distributions corresponding to unit transverse strains, and $\rho=(x_2-x_{2k})x_3^+ -(x_3-x_{3k})x_2^+ +x_{2k}G_3+x_{3k}G_2$ where x_{2k} and x_{3k} are the coordinates of the shear center. Finally, the constitutive relationships for a thin-walled beam made of laminated composite are:

$$\begin{bmatrix} n \\ q \end{bmatrix} = \begin{bmatrix} A_{nn} & A_{nq} \\ A_{nq} & A_{qq} \end{bmatrix} \begin{bmatrix} e \\ \gamma \end{bmatrix} \quad (27)$$

where the stiffness coefficients A_{ij} are related to the inplane stiffness matrix of the laminate (Tsai et al., 1983). A nonvanishing A_{nq} corresponds to inplane extension-shearing coupling for the laminate and results in elastic couplings for the beam. The total potential energy finally becomes:

$$\Pi=\frac{1}{2}\int_0^L\int_\Gamma (A_{nn}e+A_{qq}\gamma+2A_{nq}e\gamma)ds\,dz-W \quad (28)$$

This expression can be used as a basis for a finite element approximation of the problem.

4 The Strain-Displacement Expressions

In the derivation of the strain expressions (17)–(19), no assumptions were made about the magnitude of the displacements, rotations, or strains, hence, these expressions are valid for beams with small initial curvatures undergoing arbitrarily large displacements, rotations, and strains. On the other hand, in the derivation of the total potential energy expression (28), strain components were assumed small enough to render negligible changes in area due to deformation, and to equate Green-Lagrange to engineering strains. This requires both axial and shearing strains to be much smaller than unity, i.e., $e \ll 1$, and $\gamma \ll 1$; however, nothing is assumed about the relative magnitude of e versus γ. For consistency, the same assumptions must now be introduced into the strain-displacements equations (17)–(19), to obtain:

$$\begin{aligned} \epsilon_{11}= {} & \bar{e}_{11}-x_2\kappa_3+x_3\kappa_2 \quad +\delta' W_1+\delta k_1(x_3W_{1,2}-x_2W_{1,3}) \\ & +1/2(2\bar{e}_{12}-x_3\kappa_1)^2+1/2(2\bar{e}_{13}+x_2\kappa_1)^2; \end{aligned} \quad (29)$$

$$\gamma_{12}=2\bar{e}_{12}-x_3\kappa_1 \quad +\delta W_{1,2}+2\hat{e}_{12}W_{2,2}+2\hat{e}_{13}W_{3,2}; \quad (30)$$

$$\gamma_{13}=2\bar{e}_{13}+x_2\kappa_1 \quad +\delta W_{1,3}+2\hat{e}_{12}W_{2,3}+2\hat{e}_{13}W_{3,3}. \quad (31)$$

The last term appearing in equation (19) is negligible since it represents the square of the axial strain components due to bending. If we now introduce the additional assumption that axial and shearing strains are of the same order of magnitude, then $\gamma^2 \ll e$, and the two last terms of equation (29) can be neglected, since they are square of the shearing strain component (30) and (31), respectively; this yields:

$$\begin{aligned} \epsilon_{11} &= \bar{e}_{11} - x_2\kappa_3 + x_3\kappa_2 \quad &+\delta' W_1 + \delta k_1(x_3 W_{1,2} - x_2 W_{1,3}) \\ \gamma_{12} &= 2\bar{e}_{12} - x_3\kappa_1 \quad &+\delta W_{1,2} + 2\hat{e}_{12} W_{2,2} + 2\hat{e}_{13} W_{3,2}; \\ \gamma_{13} &= 2\bar{e}_{13} + x_2\kappa_1 \quad &+\delta W_{1,3} + 2\hat{e}_{12} W_{2,3} + 2\hat{e}_{13} W_{3,3} \end{aligned} \tag{32}$$

These expressions are often successfully used as the basis for beam models involving large displacements and rotations, but small strains (Rosen et al., 1979, 1987; Bauchau et al., 1987b, 1987c; Washizu, 1964). However, it is interesting to note that one additional assumption was required ($\gamma^2 \ll e$), that might not be adequate when dealing with highly anisotropic composite materials.

The seven unknown functions of the problem are the three displacements, the three rotation parameters implicitly defined in the rotation matrix T (in this effort the Euler angles were selected), and the magnitude of the torsional warping δ. These functions can be discretized using standard finite element techniques, and in this study, four noded elements (cubic interpolation functions) were used. The resulting expression for the total potential energy is strongly nonlinear since it depends on powers of the displacement functions, and products of trigonometric functions of the Euler angles. A Newton-Ralphson technique was used to iteratively solve the resulting finite element equations.

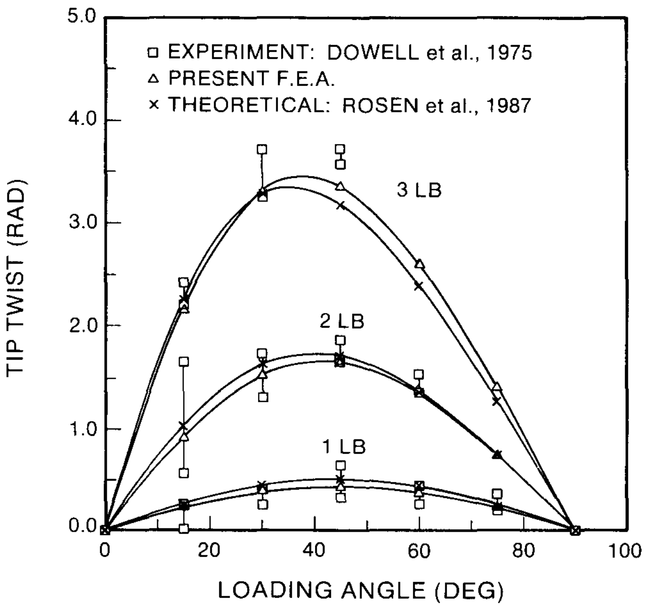

Fig. 2(a) Tip twist angle

5 Numerical Examples

The first example was selected to demonstrate the ability of the program to deal with arbitrarily large displacements and rotations; the finite element results will be compared with experimental measurements obtained by Dowell and Traybar (1975) for a slender, cantilevered beam with a solid aluminum rectangular cross section subjected to a tip load P. The angle Φ_0 between the loading direction and the major axis of the cross section (the "loading angle") can be varied from 0 to 90 deg in the experimental set-up, yielding a wide range of nonlinear problems where torsion and bending are coupled. Figures 2(*a*), (*b*), and (*c*) show the tip twist angle, the flatwise tip displacement (i.e., the displacement perpendicular to the major axis of the cross section), and the edgewise tip displacement (parallel to the major axis), respectively, versus the loading angle, for three values of the tip load ($P = 1$, 2, and 3 lbs). In all cases excellent correlation is found between the finite element predictions, a theoretical prediction by Rosen et al. (1987), and the experimental results. The strain fields (29)–(31) or (32) gave identical predictions.

The following examples all deal with the extension-twisting behavior of composite beams. This problem is important for helicopter blade analysis since large axial centrifugal loads are present in the blade, and small changes in torsional stiffness result in angle of attack variations that could in turn result in large changes in the blade's aerodynamic loading. Moreover, any coupling between extension and twisting could have a stabilizing or destabilizing effect on the blade's behavior. This is especially important in the design of a flexbeam, that structure connecting the blade's root to the rotor hub. The flex-

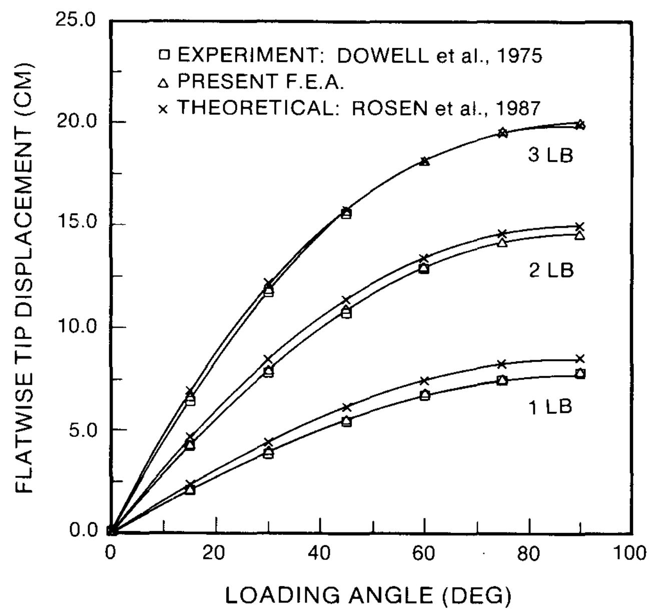

Fig. 2(b) Flatwise tip displacement

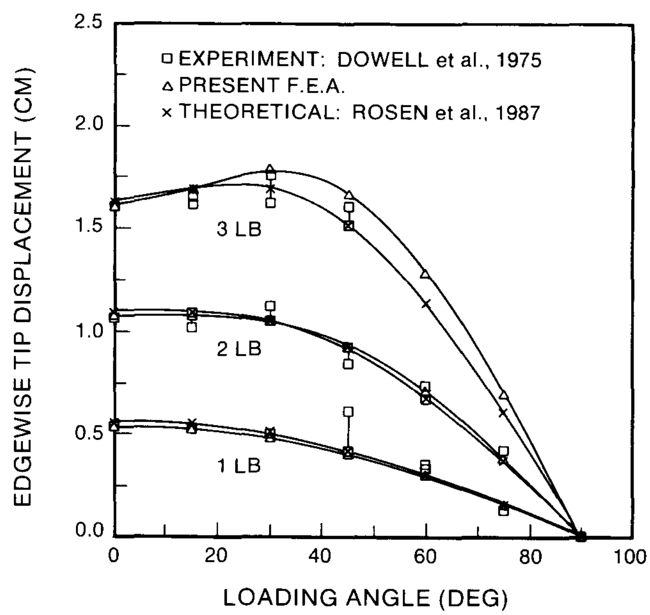

Fig. 2(c) Edgewise tip displacement

Fig. 2 Tip displacements of the beam versus loading angle

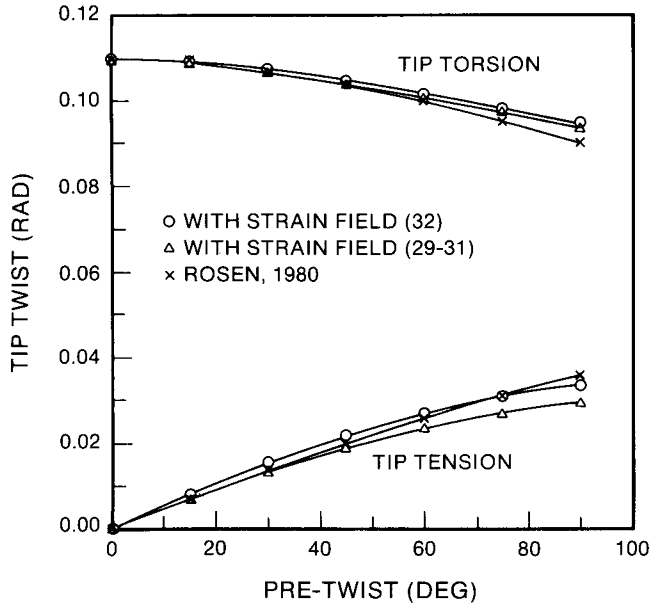

Fig. 3 Tip twist of a thin-walled box beam versus pretwisting angle

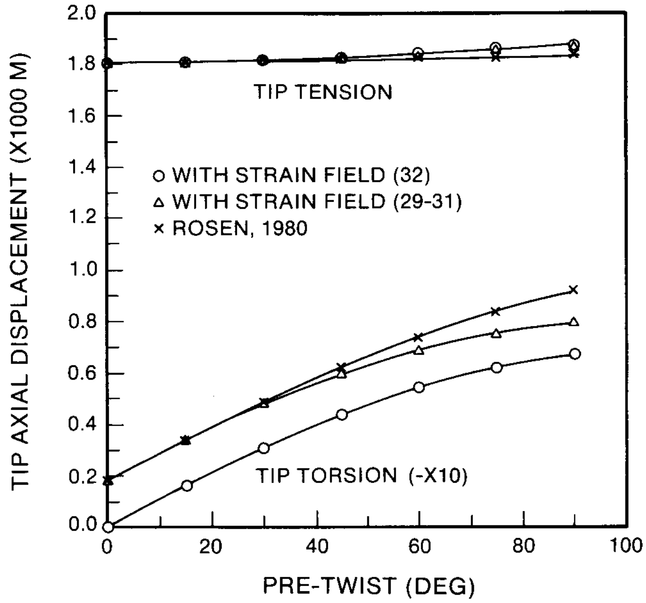

Fig. 4 Tip displacement of a thin-walled box beam versus pretwisting angle

beam must have a very high axial strength (to carry the centrifugal load) together with very low torsional stiffness (to allow easy control of the blade's pitch). This results in a highly anisotropic structure prone to extension twisting coupling, and extremely sensitive to such coupling.

Extension-twisting coupling can originate from three sources. First, naturally twisted beams will tend to untwist under an axial load; this effect is purely linear and results from differential torsional warping (Rosen, 1980), hence the importance of including this warping effect in the analysis. Second, a straight beam will tend to stiffen under an applied axial load. This effect is independant of warping and will occur even for a circular cross section which exhibits no torsional warping. It is a nonlinear effect due to the square shearing strain term discussed in equations (32); this term is generally small, however it can become significant for highly anisotropic beams. Finally, extension-twisting coupling can result from elastically tailoring a composite lay-up to that effect. This is a linear effect originating from a nonvanishing A_{nq} (27).

To demonstrate the first effect, the torsional behavior of a naturally twisted rectangular box beam under tip torque and axial load is analyzed. The cross-sectional width and height are 127.0 and 25.4 mm, respectively, the beam's length is 0.635 m. The thin walls consist of a laminated Graphite/Epoxy composite with a $[0_2^\circ, \pm 15^\circ]_s$ lay-up corresponding to stiffness coefficients $A_{nn} = 115.0$ MN/m, $A_{qq} = 8.5$ MN/m, and $A_{nq} = 0$, and a wall thickness of 1 mm. The upper curve of Fig. 3 shows the tip twist under a fixed tip torque as a function of the initial pretwist angle, and the lower curve shows the tip twist under a fixed axial load. Figure 4 shows the tip displacement under the same conditions. Note the torsional stiffening under tip torque, and the "untwisting" under tip tension, which are linear effects. The choice of the strain field (29)-(31) versus equations (32) has a minimum effect on the major displacement component (i.e., displacement under tip load or twist under tip torque), but a more significant effect on the coupled displacement components (twist under tip load and displacement under tip torque). The results are in good agreement with theoretical predictions by Rosen (1980). Note that Rosen also included the shearing strain square term in his analysis (i.e., strain field (29)-(31)). The discrepancy between the present analysis and Rosen's results at large pretwist angles comes from the fact that in the latter analysis the amplitude of the torsional warping displacement is chosen proportional to the twist rate, but is an independant quantity in the present analysis resulting in a greater flexibility of the beam.

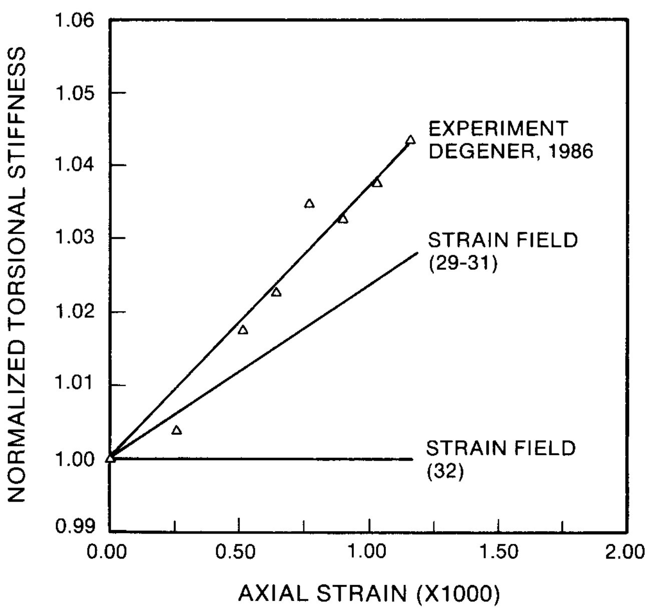

Fig. 5 Normalized torsional stiffness of a Kevlar Beam under axial tension

Consider next a thin-walled Kevlar beam ($L = 0.6$ m) with a circular cross section (outer diameter is 6 mm, and the wall thickness is 0.125 mm); the lay-up consists of unidirectional fibers aligned with the axis of the beam, and the stiffness coefficients are $A_{nn} = 8.25$ MN/m, $A_{qq} = 0.35$ MN/m, and $A_{nq} = 0$. In an experimental study (Degener, 1986) the torsional stiffness of this beam was measured for various levels of applied axial strain. Figure 5 shows the measured torsional stiffness (normalized by the initial torsional stiffness) versus the axial strain. A model of this problem based on the strain field (32) predicts a constant torsional stiffness, in contrast with the observed experimental results. For this simple case, the strain field (32) reduces to:

$$\epsilon_{11} = \bar{e}_{11} \text{ and } \gamma = \rho \kappa_1, \tag{29}$$

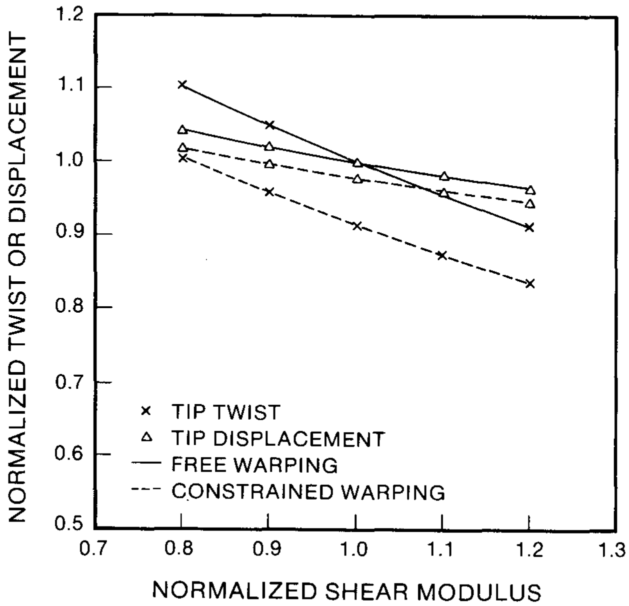

Fig. 6 Normalized tip twist and displacement of a rectangular box beam with extension-twisting couplings, under tip tension

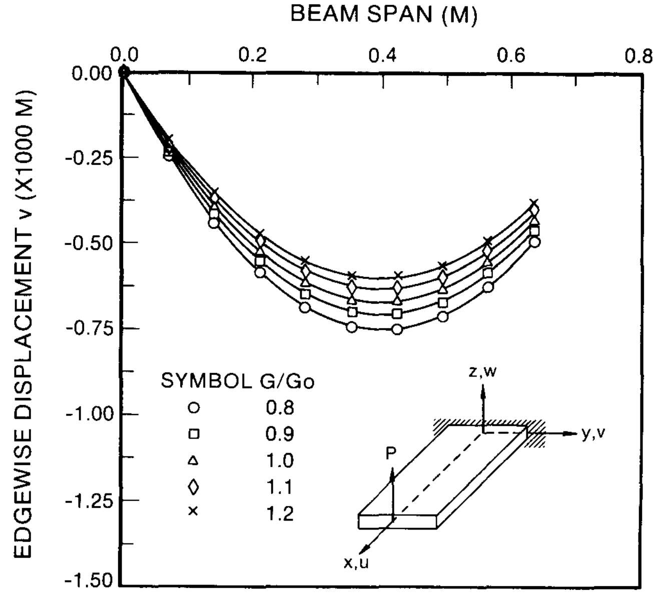

Fig. 7 Edgewise displacement of a rectangular box beam with extension-twisting couplings, under tip transverse load

which clearly show that axial and shearing strains are uncoupled. On the other hand, the strain field (29)-(31) gives:

$$\epsilon_{11} = \bar{e}_{11} + \frac{1}{2}\rho^2\kappa_1^2 \text{ and } \gamma = \rho\kappa_1, \tag{30}$$

which now exhibits a kinematic coupling term between tension and torsion. The strain energy then becomes:

$$U = \frac{1}{2}\int_0^L \int_\Gamma [A_{nn}(\bar{e}_{11} + \frac{1}{2}\rho^2\kappa_1^2)^2 + A_{qq}\rho^2\kappa_1^2] ds\, dx \tag{31}$$

and neglecting the term in κ_1^4 the torsional stiffness GJ becomes:

$$GJ = A_{qq} I_p (1 + e_{11} A_{nn}/A_{qq}). \tag{32}$$

Where I_p is the polar moment of inertia of the cross section. In this expression the dependency of the torsional stiffness on the axial strain level clearly appears. For most isotropic and homogeneous engineering materials Poisson's ratio is about 0.3, hence the ratio $A_{nn}/A_{qq} = 2.6$, and GJ remains virtually constant for small axial strain levels. However, for anisotropic materials this ratio could be much larger (about 24 for unidirectional Kevlar) resulting in a significant increase in torsional stiffness.

Figure 5 shows that the predictions based on the strain field (29)-(31) are in closer agreement with the experimentally measured torsional stiffnesses which increased of about 4 percent for an axial strain of 1000 μm/m. In a typical flexbeam, the axial strain level would be significantly higher (about 5000 μm/m) resulting in drastic torsional stiffness changes. It is also important to note that the additional strain term introduces a kinematic coupling between extension and twisting that is inexistent when this term is neglected. Such a coupling could potentially affect the stability of the blade. The observed discrepancy between the experimental results and the present calculations might be due to simplified material constitutive relationship used in this model (however, Kevlar exhibits a linear stress-strain curve in the fiber direction for $e \leq 1000$ μm/m, and the shearing strain was kept below 50 μm/m during the experiment).

The last example involves a composite beam exhibiting elastic couplings. The geometry is once again a thin-walled rectangular box section of dimensions given above. The web has the following stiffness parameters: $A_{nn} = 90.3$ MN/m, $A_{qq} = 23.3$ MN/m, and $A_{nq} = 0$, corresponding to a $[\pm 45 \text{ deg}]_s$ lay-up of a T300/5208 Graphite/Epoxy composite (0 deg corresponds to fibers aligned with the axis of the beam). Two different flange configurations were considered: in the first case both upper and lower flanges consist of a $[15_2, 0, 30]_s$ lay-up, resulting in extension-twisting coupling (stiffness parameters are $A_{nn} = 119.4$ MN/m, $A_{qq} = 14.1$ MN/m, and $A_{nq} = 22.5$ MN/m). In the second case the lay-ups are $[15_2, 0, 30]_s$ and $[-15_2, 0, -30]_s$, for the upper and lower flanges, respectively, resulting in bending-twisting coupling.

This beam will be used as a rough model of an elastically tailored helicopter blade; two important features of such structures will be illustrated. The first feature is the marked dependency of their bending and torsional behavior on the ply shearing modulus G_{LT} (Shyprykevitch, 1982). Whenever possible, a designer will select the composite lay-up that optimizes strength or stiffness by taking advantage of the high strength and stiffness in the fiber direction, hence minimizing the effect of ply shearing and transverse properties on overall laminate behavior. However, elastic coupling in a thin-walled beam is obtained through extension-shearing coupling of the laminate which is itself strongly dependent on G_{LT}, hence, it is not possible to obtain elastic couplings without a strong dependency on this modulus. To illustrate this point the behavior of coupled beams will be presented as a function of normalized ply shearing modulus, where the normalization factor is chosen as the nominal G_{LT}. The second feature is the more pronounced dependency of the overall behavior on nonclassical effects of beam theory such as torsional warping constraints.

Figure 6 shows the normalized tip twist the displacement under tip axial load of 100 KN for the beam with extension-twisting couplings (this would model the effect of centrifugal loads on a helicopter blade). Two types of boundary conditions are considered at the root: the torsional warping is either free or constrained. As expected, both normalized G_{LT} and torsional warping significantly affected the torsional behavior of the beam, however, the same factors also affect the extensional behavior, though less significantly.

Another important point is that this lay-up, designed to exhibit extension-twisting coupling, will also present several other types of couplings; consider the same beam under a tip-

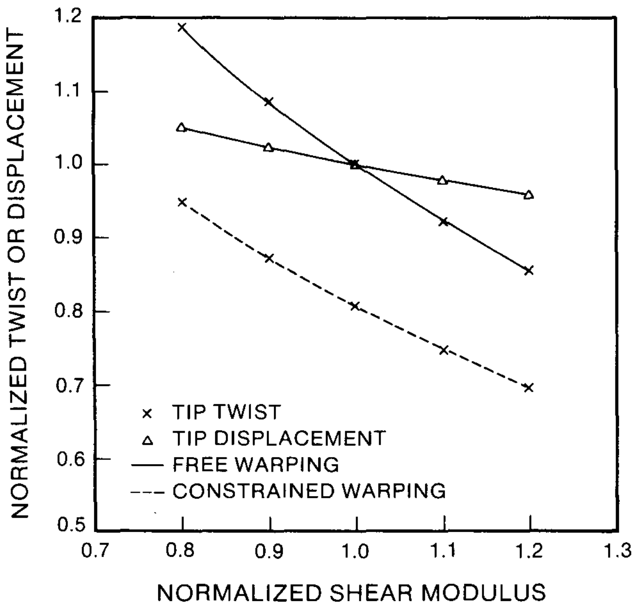

Fig. 8 Normalized tip twist and displacement of a rectangular box beam with extension-twisting couplings, under tip transverse load

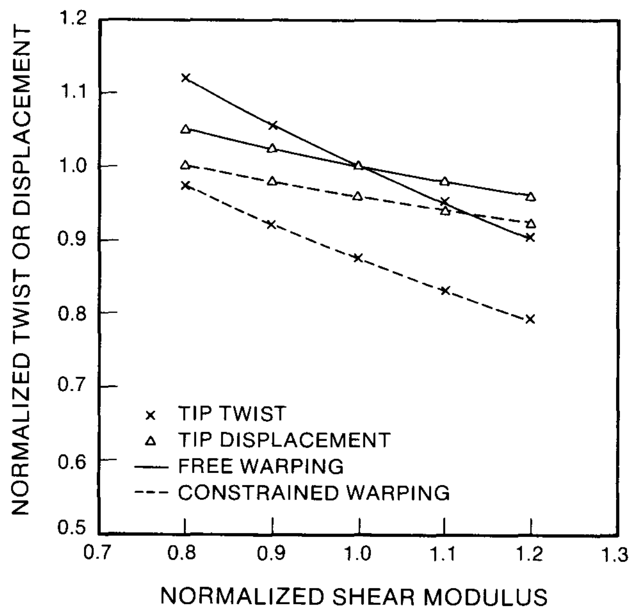

Fig. 9 Normalized tip twist and displacement of a rectangular box beam with bending-twisting coupling, under tip transverse load

flatwise load $P = 1$ KN (this would model the lift force on the blade). Figure 7 shows the resulting edgewise displacement v. This load generates a uniform shear force over the span of the beam, and a linearly varying bending moment. This bending moment couples with edgewise shearing to generate negative v displacements, and is dominant near the root of the beam. On the other hand, the shear force couples with bending about the y axis to generate positive v displacements, and is dominant near the tip of the beam where the bending moment vanishes. This explains the deformed shape of the beam shown in Fig. 7. This coupling between flatwise and edgewise motions is of importance to helicopter blade stability because of the very different aerodynamic damping characteristics for these two types of motion. In these examples, the strain fields (29)–(31) or (32) gave identical predictions.

When nonlinear effects are taken into account, the edgewise motion v displaces the point of application of the load P, causing twisting of the beam. Figure 8 shows this tip twist and the w displacement versus the normalized shear modulus. Torsional warping significantly affect the tip twist (about 20 percent) but has no effect on the axial displacements (the two curves superpose on Fig. 8), and both tip twist and displacement vary with G_{LT}.

Finally the behavior of the beam with bending-twisting couplings is shown in Fig. 9. Once again, both tip twist and displacement are affected by torsional warping and ply shearing modulus.

7 Conclusions

This paper has presented a consistent formulation for the modeling of beams with small initial curvature undergoing arbitrarily large displacements and rotations but small strains. Transverse shearing deformations, torsional warping effects, and elastic couplings resulting from elastically tailored composite beams were included in the analysis. Numerical results based on a finite element approximation of the resulting equations were presented. These examples focused on the extension-twisting behavior of beams as it impacts the design of helicopter composite blades.

The extension-twisting coupling of a pretwisted beam due to torsional warping is included in the model and is in agreement with previous modeling of this effect. Next, a shearing strain square term was shown to affect the behavior of beams with pronounced anisotropy. This nonlinear effect is usually neglected in small strain analyses, however it introduces a kinematic coupling between extension and twisting that should be important for the design and stability of helicopter flexbeam attachments. Finally elastic tailoring of helicopter blades is an increasingly important issue for performance optimization, however some important facts should be noted. First, multiple coupling terms are likely to be present, for instance beam exhibiting extension-twisting or bending twisting couplings will often present bending-transverse shearing or transverse shearing-warping couplings that affect the overall behavior of the structure. Second, several nonclassical effects of beam theory become more prevalent on the overall behavior; for instance torsional warping constraints are known to affect the torsional behavior of a beam, however, when the beam exhibits elastic couplings, torsional warping constraints will also significantly affect bending and axial behavior. Finally, the material shearing modulus also becomes an important factor affecting not only torsional, but axial and bending behavior as well.

Acknowledgments

This research was sponsored by the Army Research Office under Grant DAAG 29-82-K-0093, and Dr. Robert Singleton was contract monitor.

References

Bathe, K. J., 1982, *Finite Element Procedures in Engineering Analysis*, Perentice-Hall, Englewood Cliffs, NJ.

Bauchau, O. A., 1985, "A Beam Theory for Anisotropic Materials," ASME Journal of Applied Mechanics, Vol. 107, pp. 416–422.

Bauchau, O. A., Coffenberry, B. S., and Rehfield, L. W., 1987a, "Composite Box Beam Analysis: Theory and Experiments," *J. Reinforced Plastics and Composites*, Vol. 6, No. 1.

Bauchau, O. A., and Hong, C. H., 1987b, "Finite Element Approach to Rotor Blade Modeling," *J. Amer. Hel. Soc.*, Vol. 32, No. 1, pp. 60–67.

Bauchau, O. A., and Hong, C. H., 1987c, "Large Displacement Analysis of Naturally Curved and Twisted Composite Beams," *J. AIAA*, Vol. 25, No. 10.

Degener, M., 1986, "Experimental Investigation of the Torsional Stiffness of a Composite Beam Under Axial Loading," Report of DFVLR Institute of Aeroelasticity.

Dowell, E. H., and Traybar, J. J., 1975, "An Experimental Study of the

Nonlinear Stiffness of a Rotor Blade Undergoing Flap, Lag, and Twist Deformations," Princeton University, Aerospace and Mechanical Science Report No. 1257.

Friedmann, P. P., 1977, "Recent Developments in Rotary-wing Aeroelasticity," *J. Aircraft*, Vol. 14, No. 11, pp. 1027–1041.

Rosen, A., and Friedmann, P. P., 1979, "The Nonlinear Behaivor of Elastic Slender Straight Beams Undergoing Small Strain and Rotations," ASME Journal of Applied Mechanics, Vol. 46, pp. 161–168.

Rosen, A., 1980, "The Effect of Initial Twist on the Torsional Rigidity of Beams: Another Point of View," ASME Journal of Applied Mechanics, Vol. 47, pp. 389–392.

Rosen, A., Loewy, R. G., and Mathew, M. B., 1987, "Nonlinear Analysis of Pretwisted Rods Using 'Principal Curvature Transformation'—Part I—Theoretical Derivation, Part II—Numerical Results," *AIAA J.*, Vol. 25, No. 3, pp. 470–478.

Shyprykevich, P., 1982, "Characterization of Advanced Composite Laminates for Aeroelastic Tailoring," Grumman Aerospace Corporation, Report NAS 1-14759.

Tsai, S. W., and Hahn, H. T., 1983, *Introduction to Composite Materials*, Technomic Publishing Co.

Washizu, K., 1975, *Variational Methods in Elasticity and Plasticity*, Pergamon Press, Elmsford, NY.

Washizu, K., 1964, "Some Considerations on a Naturally Curved and Twisted Slender Beam," *J. Math and Phys.*, Vol. 48, No. 2, pp. 111–116.

Wempner, G., 1981, *Mechanics of Solids with Application to Thin Bodies*, Sijthoff and Noordhoff.